

www.acsanm.org Article

On the Origin of Nonclassical Ripples in Draped Graphene Nanosheets: Implications for Straintronics

Riju Banerjee,* Tomotaroh Granzier-Nakajima, Aditya Lele, Jessica A. Schulze, Md Jamil Hossain, Wenbo Zhu, Lavish Pabbi, Malgorzata Kowalik, Adri C. T. van Duin, Mauricio Terrones, and E. W. Hudson*



Cite This: ACS Appl. Nano Mater. 2022, 5, 10829-10838



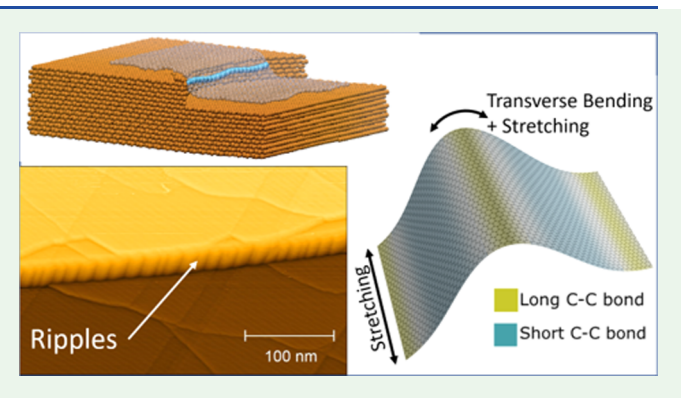
ACCESS

Metrics & More

Article Recommendations

s Supporting Information

ABSTRACT: Ever since the discovery of graphene and subsequent explosion of interest in single-atom-thick materials, studying their mechanical properties has been an active area of research. Atomistic length scales often necessitate a rethinking of physical laws, making such studies crucial for understanding and ultimately utilizing material properties. Here, we report on the investigation of nanoscale periodic ripples in suspended, single-layer graphene sheets by scanning tunneling microscopy and atomistic scale simulations. Unlike the sinusoidal ripples found in classical fabrics, we find that graphene forms triangular ripples, where bending is limited to a narrow region on the order of a few unit cell dimensions at the apex of each ripple. This nonclassical bending profile results in graphene behaving like a bizarre fabric,



which regardless of how it is draped, always buckles at the same angle. Investigating the origin of such nonclassical mechanical properties, we find that unlike a thin classical fabric, both in-plane and out-of-plane deformations occur in a graphene sheet. These two modes of deformation compete with each other, resulting in a strain-locked optimal buckling configuration when draped. Electronically, we see that this in-plane deformation generates pseudo electric fields creating $a \sim 3$ nm wide pnp heterojunction purely by strain modulation.

KEYWORDS: graphene, strain, nonclassical, mechanical properties, electronic properties, STM

■ INTRODUCTION

From the folds in our textiles to ripples in plastic wrap and draped tablecloths, deformations of thin sheets are common everyday occurrences. The essential physics of these everyday observations was worked out more than a century ago by Lord Rayleigh in his book Theory of Sound. Unlike familiar thin fabrics with finite measurable thicknesses, single-atom-thick two-dimensional (2D) materials are the ultimate limit of thin sheets, and understanding how they deform has been the focus of research over the past decade. From a fundamental viewpoint, it is important to understand how the mechanical properties of 2D materials, especially rippling, buckling, folding, and crumpling, differ from those of classical fabrics. From an application viewpoint, the potential to develop novel electronic devices, which exploit the ability of 2D materials to deform into complex three-dimensional structures while bending with very small radii, makes these studies crucial.²⁻⁶ One of the earliest studies of graphene's mechanical properties was done by Lee et al.7 by making indentations in suspended graphene with an atomic force microscope. They found that graphene has Young's modulus of 1 TPa (5 times that of most steels) and an intrinsic strength of 130 GPa (50 to 100 times that of most steels)—the highest for any material ever measured. On the theoretical side, efforts were also made to go beyond numerically expensive first-principles calculations toward equivalent continuum models that can explain the mechanics of larger graphene sheets as a fabric. Finding an equivalent description of 2D materials analogous to classical fabrics is challenging for two main reasons. First, the inability to properly define the plate thickness of a single atomic layer results in wide variations in bending and Young's moduli among different studies, known as Yakobson's paradox. Second, an equivalent description of a discrete lattice is challenging when the length scale of strain variation becomes comparable to the lattice constant. In particular, it is plausible that Rayleigh's theories get modified when deformation length

Received: May 17, 2022 Accepted: July 11, 2022 Published: July 26, 2022





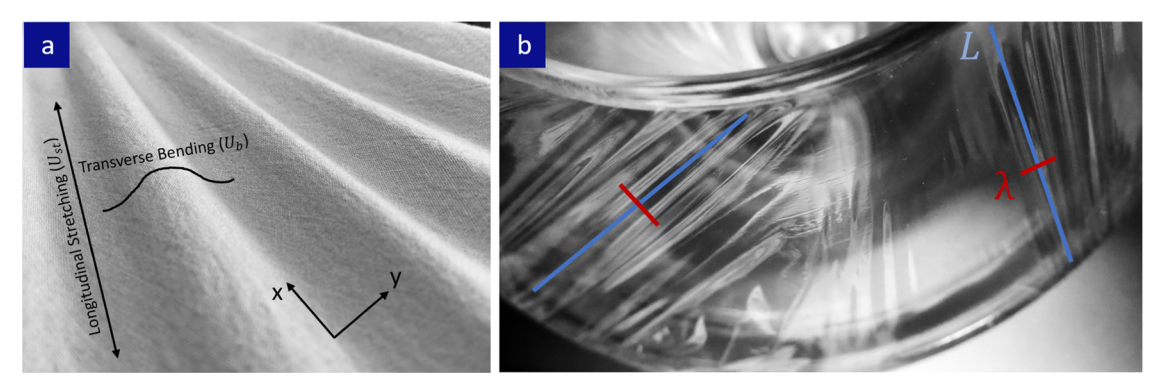


Figure 1. Rippling in classical fabrics: (a) Applying tensile stress to a fabric in the longitudinal direction (x) results in a Poisson compression in the transverse direction (y), creating ripples. The shape of ripples in a classical fabric is determined by balancing energy contributions from two deformations: stretching in the longitudinal direction (with corresponding energy cost $U_{\rm st}$) and bending in the transverse direction (energy cost $U_{\rm b}$). (b) Plastic wrap spread over two concentric cylinders, with a taller inner cylinder, also yields such tension ripples. As strain γ is kept constant, ripple wavelength λ and sheet length L follow a scaling law $L \propto \lambda^2$, as in eq 2 of the text. In the figure, ripples on the right have a smaller wavelength (red) and amplitude than those on the left. But to stabilize the larger ripples, the left ripples must run diagonally, increasing the effective sheet length L (blue).

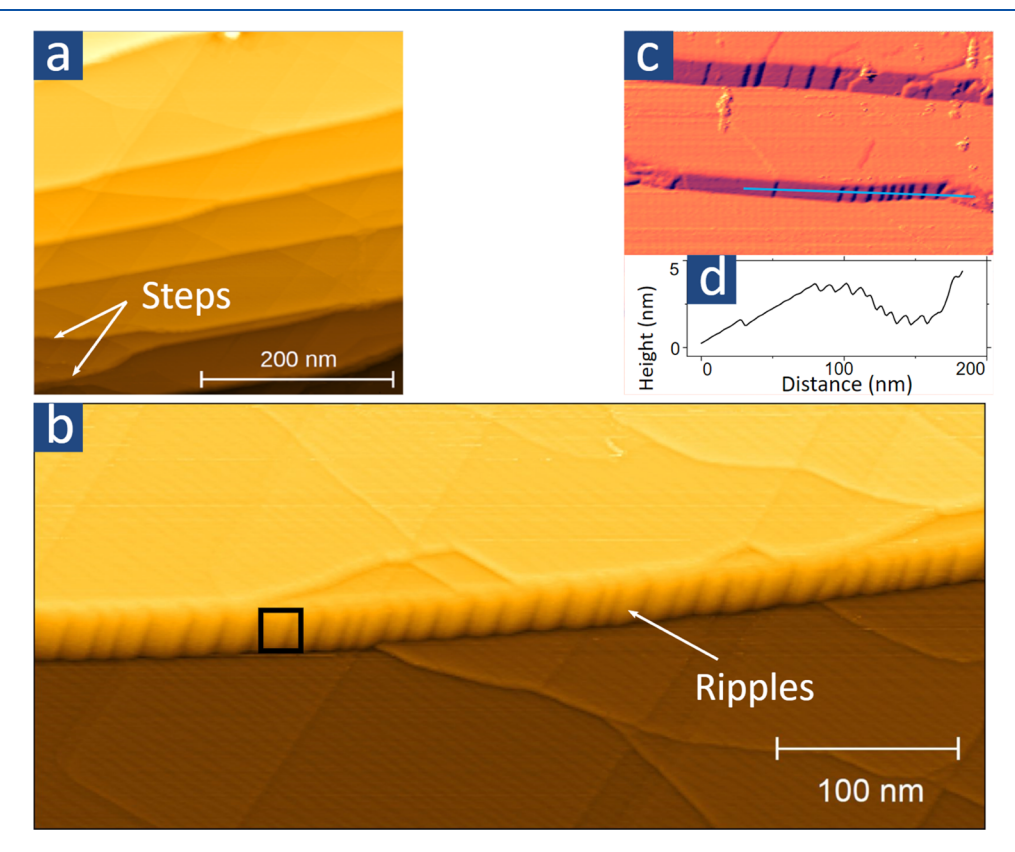


Figure 2. Creating nanoscale ripples in graphene: (a) STM topograph of graphene grown on copper with large (up to \sim 35 nm high) step edges (current setpoint $I_{\rm set}=70$ pA, sample bias $V_{\rm s}=0.1$ V; all displayed STM data in the paper is obtained at temperature T=80 K and unfiltered). (b) Magnified image of a step edge ($I_{\rm set}=80$ pA, $V_{\rm s}=0.1$ V) shows graphene draping over the step forming ripples as it is stretched by the contact forces of the Cu substrate. The black box highlights the ripple near the crest of which the spectra shown in Figure 5c are taken. The faintly visible tilted parallel lines in the flat terraces are surface reconstructions of the Cu substrate underneath graphene, as also observed by Tian et al. (c) Analogous to corners of a draped tablecloth, high-curvature regions are associated with higher ripple density (and hence smaller ripple wavelength) as highlighted in the topographic profile (d), extracted along the blue line ($I_{\rm set}=170$ pA, $I_{\rm set}=100$ pA, $I_{\rm set}=100$ pC. 12 V).

scales approach the atomic limit when electronic interactions (which were unknown when the classical theory was developed) between neighboring atoms can become important. Indeed, Tapaszto et al. ¹³ found that nanometer-length-scale graphene ripples have shapes that cannot be described by a continuum mechanics approach valid for a classical fabric. ¹⁴ Interestingly, Bai et al. ¹⁵ found that this discrepancy persists for

ripples measuring up to 100 nm, length scales much larger than the lattice constant, whereas micron-sized ripples were well described by continuum mechanics. This suggests two regimes in which ripples in graphene follow different sets of laws. Continuum mechanics describes well graphene ripples with a wavelength of around 1 micron and greater, and another unknown set of laws governs the rippling of graphene on the

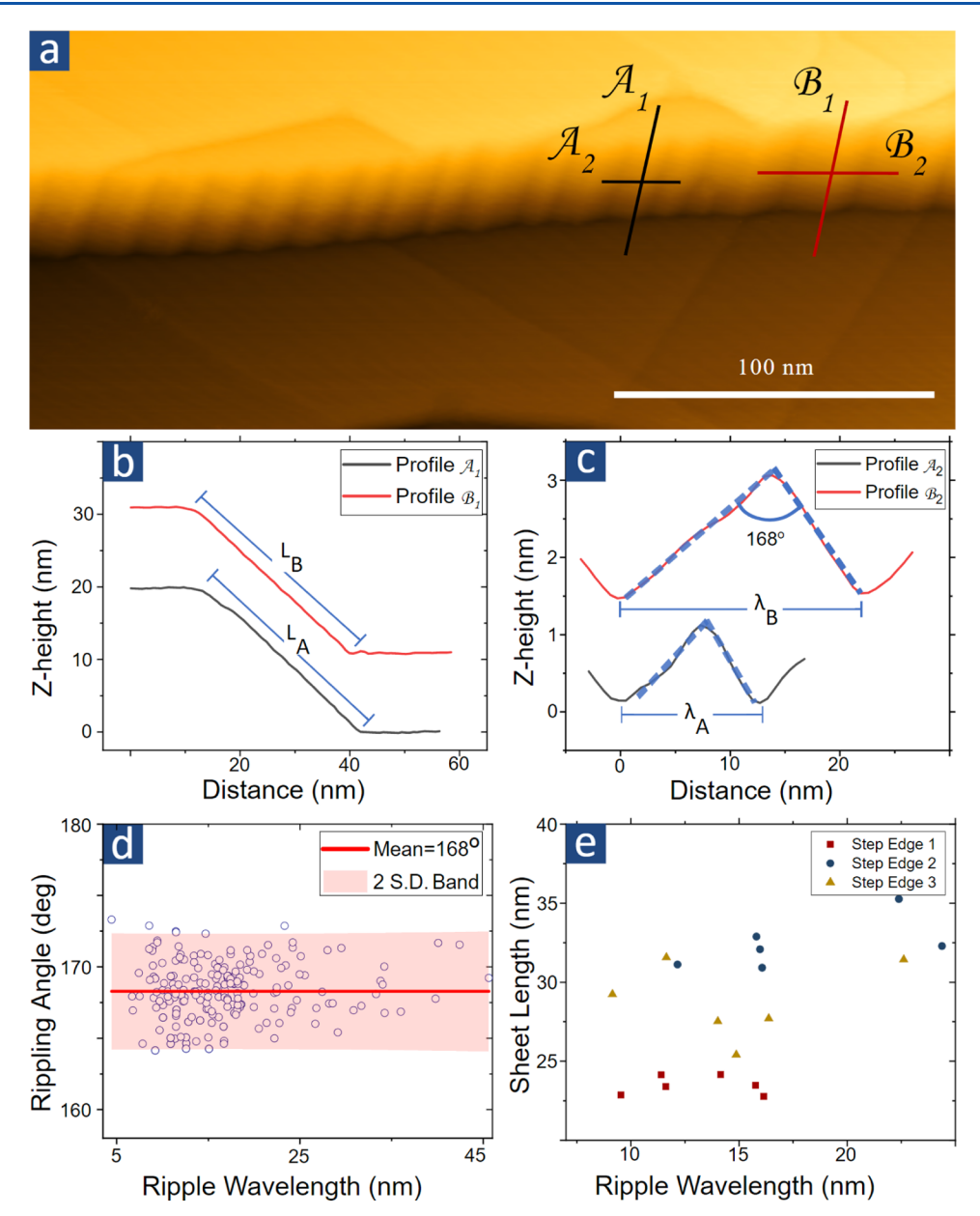


Figure 3. Shape of graphene: (a) topography of ripples on draped graphene ($I_{\text{set}} = 30 \text{ pA}$, $V_{\text{s}} = 0.1 \text{ V}$) from whence we extract profiles (b) down the sheet ($\mathcal{A}_1/\mathcal{B}_1$), revealing sheet length, and (c) along the sheet ($\mathcal{A}_2/\mathcal{B}_2$), showing ripple wavelength and the apex angle. Dashed lines highlight the triangular shape. Profiles are offset for clarity and have different scales for the horizontal and vertical axes. (d) Rippling angle is conserved at 168° ($\pm 3^{\circ}$), independent of step height and curvature, ripple amplitude, and wavelength (pictured here, with two standard deviation ranges shaded pink). (e) Measurements of sheet length and ripple wavelength from three separate step edges show the violation of classical scaling, which predicts $L \propto \lambda^2$.

length scales below 100 nm. Here, we investigate the origin of the latter, with graphene ripple wavelengths on the order of tens of nanometers.

Ripples are necessary for the stability of 2D materials^{17–19} and are commonly observed in scanning tunneling microscopy (STM) investigations of graphene. However, the development of a thorough formalism of 2D material deformation at the nanoscale, equivalent to that for classical fabrics, has been hindered due to the difficulty of creating reproducible nanoscale ripples such that physically relevant parameters like wavelength, amplitude, sheet length, and curvature can be systematically varied and measured over a large parameter space. Instead, experimental studies have typically relied on the good fortune of finding wrinkles in 2D materials. ^{15,20–25}

Though it is possible to induce controlled strain by patterning substrates, ^{26–28} this approach tends to create wrinkles with deformation length scales much larger than the lattice spacing. In contrast to these traditional approaches, we develop a technique to create reproducible nanoscale ripples by draping graphene over Cu step edges and experimentally investigate a large parameter space of wavelengths, amplitudes, and sheet lengths.

In describing the deformation of a classical sheet, Rayleigh argued¹ that there are two ways a uniform isotropic thin sheet can deform: out-of-plane bending and in-plane stretching. When a sheet of thickness t bends with a radius of curvature R, then the strain due to bending, γ_b , varies through its thickness as $\gamma_b \sim z/R$ where z is the axis normal to the sheet surface.

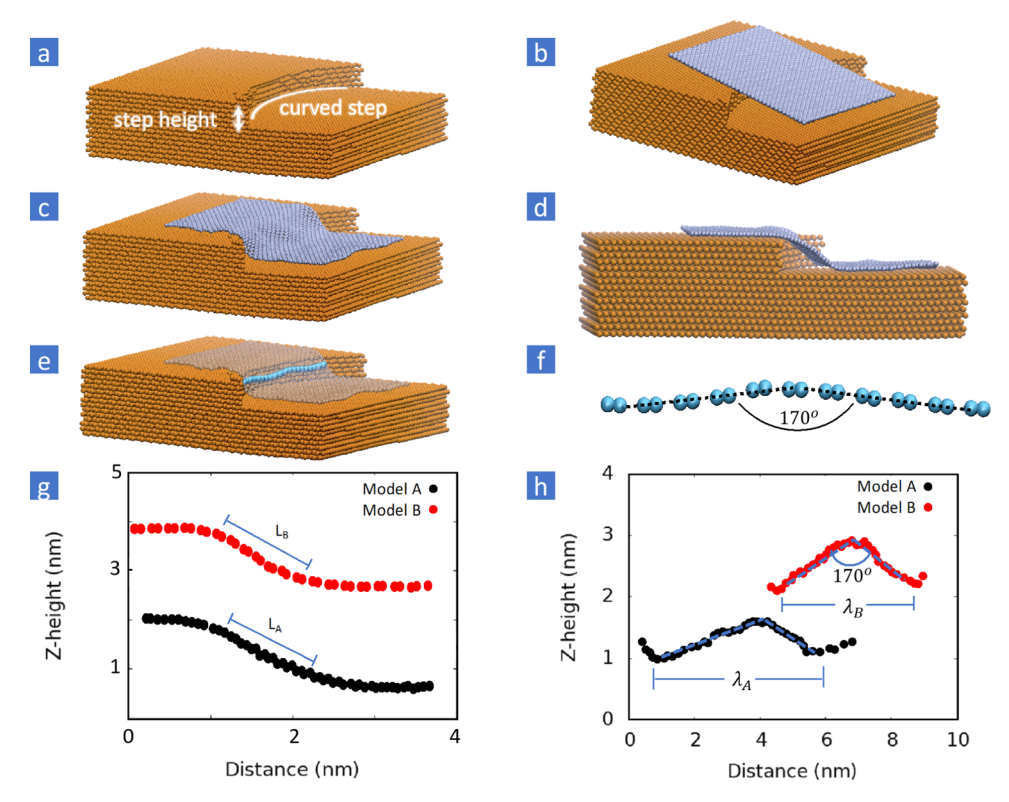


Figure 4. Atomistic scale simulations: building process and simulation results for an atomistic representation of a curved Cu step with rippled, suspended graphene. To investigate formation of ripples in graphene draped over a curved Cu step edge (a), we place a sheet of graphene in close proximity to this Cu step (b) and let the system relax to form rippled, suspended graphene (c). Cut along the crest of the ripple, showing only half the system is presented in (d), while the ripple profile can be seen in the highlighted cyan atom chain (e) and in an extracted profile showing the apex angle (f). Profiles obtained from the final structure for two models with different Cu step radii of curvature (model A: 10 nm; model B: 15 nm; see the Supporting Information, Section 3) (g) down the sheet reveal sheet length and (h) along the sheet show ripple wavelength and apex angle. The profiles are offset for clarity.

Hence, the energy density due to bending, $U_{\rm b}$, is $U_{\rm b} \sim \int \gamma_b^2 \, {\rm d}z$ $\sim t^3$. Similarly, the energy density due to a uniform stretch is $U_{\rm st} \sim \int \gamma_{\rm st}^2 \, {\rm d}z \sim t$. Thus, the total energy U due to deformation is

$$U \sim t^3$$
(bending) + t (stretching) (1)

As the deformation should minimize energy cost, Rayleigh remarked 'when the thickness is diminished without limit, the actual displacement will be one of pure bending'. Scaling laws relating wavelength, sheet length, and strain magnitude for a thin classical rippled sheet were deduced by Cerda and Mahadevan. In particular, they showed that ripples in a classical fabric (Figure 1a) obey the scaling law relating wavelength λ , strain γ , sheet length L, and thickness t

$$L \sim \frac{\sqrt{\gamma} \lambda^2}{t} \tag{2}$$

This scaling law implies that for a sheet under constant strain, the sheet length L varies as λ^2 . An example of this is illustrated in Figure 1b, where the ripples on the left have a larger wavelength and amplitude than those on the right, but to accommodate the larger ripples, the sheet must drape down diagonally, effectively increasing the sheet length. We sketch the origin of this scaling law in the Supporting Information, Section 9.

RESULTS

For most STM studies of graphene, an atomically flat substrate is desired to facilitate the growth of large grains and to ease scanning. However, to encourage the rippling of graphene in our study, we grow graphene via low-pressure chemical vapor deposition at a high temperature (1020 °C) on an electropolished Cu substrate (see the Supporting Information, Section 1). Under these growth conditions, step bunching leads to the formation of large steps up to 35 nm tall (Figure 2a). Graphene drapes down these large steps forming ripples (Figure 2b) in the draped (suspended) regions.

These ripples occur preferentially in regions of higher step edge curvature (Figure 2c,d). This is analogous to the classical case of ripples forming at the corners of a tablecloth, a result of having more expendable materials at that location. In Figure 3, we present measurements of their wavelength, amplitude, and sheet length. The wide variation of parameters from more than 200 independent measurements across multiple steps enables us to explore a large parameter space. This, in turn, allows us to avoid the necessity of estimating experimentally unmeasured quantities like the effective thickness of the graphene sheet and its Poisson's ratio at the nanoscale ^{13,15} and instead look for scaling relationships to directly test classical laws (Figure 3).

Figure 3c shows that contrary to a sinusoidal profile of ripples observed in classical fabrics, these ripples have a triangular shape. The technique to extract linecuts from draped graphene regions is detailed in the Supporting Information, Section 7. More interestingly, all ripples have the same bending

angle at the vertex, 168° ($\pm 3^{\circ}$), consistent across order of magnitude variations in wavelength (Figure 3d), amplitude, and step height. This conserved bending angle means that the ripple's wavelength is proportional to its amplitude. Such a situation arises in the classical theory for ripples with uniform strain due to transverse inextensibility. A sheet that is stretched in the longitudinal direction with strain γ Poisson contracts in the transverse direction. The transverse inextensibility of the sheet implies that when a flat region of width λ' buckles forming a ripple of wavelength λ and amplitude A, then they are related by $\left(\frac{\lambda'}{2}\right)^2 \approx \left(\frac{\lambda}{2}\right)^2 + A^2$. The contraction in the transverse direction due to this out-of-plane buckling is $\Delta \lambda = \lambda' - \lambda \approx \frac{2A^2}{\lambda}$ for $\Delta \lambda \ll \lambda$. As this contraction results in the Poisson compression, we have $\gamma_{\rm transverse} = \nu \gamma = \frac{\Delta \lambda}{\lambda} = \frac{2A^2}{\lambda^2}$, where ν is Poisson's ratio. Thus, we have $A \propto \sqrt{\gamma} \lambda$, as also derived in ref 14. We also note that triangular deformations like these were also predicted using molecular dynamics simulations when graphene is placed in a

These two scaling laws, viz., $A \propto \sqrt{\gamma} \lambda$ and $L \sim \frac{\sqrt{\gamma} \lambda^2}{4}$ (eq 2), imply that for any two arbitrary ripples in a classical fabric, only two scenarios are possible: either (i) γ is the same, in which case both $A \sim \lambda$ and $L \sim \lambda^2$ or (ii) γ is different, in which case neither $A \sim \lambda$ nor $L \sim \lambda^2$. As we observe a conserved bending angle at the crest of each ripple (Figure 3d), the ripples satisfy the scaling relation $A \sim \lambda$. If the observed ripples are classical, then from case (i) above, they must also satisfy $L \sim \lambda^2$. We test this prediction directly by measuring sheet length L and wavelength λ of ripples. Figure 3a displays two regions on the same step where measurements were taken. For these two regions, the local ripple wavelengths, shown in Figure 3c along the ripple direction \mathcal{A}_2 and \mathcal{B}_2 , differ by a factor of 2 ($\lambda_{\rm B} \approx$ $2\lambda_A$), while the sheet lengths (Figure 3b) are nearly identical, $L_{\rm B} \approx L_{\rm A}$ in strong contrast with the classical prediction of $L_{\rm B} \approx$ $4L_A$ (from eq 2). A plot of sheet length versus wavelength for several ripples observed on three different step edges (Figure 3e) highlights the lack of any clear correlation between the two variables. The disagreement between scaling laws predicted by the classical theory of rippling and our measurements demonstrates that the classical theory is not valid for nanoscale ripples in graphene. We also note a potential caveat that the classical scaling law $L \propto \lambda^2$ is strictly valid for a flat geometry, but the ripples were observed on curved step edges, and whether that can invalidate our arguments showing graphene to be nonclassical. We address this issue in the Supporting Information, Section 9, where we show that as the local radius of curvature of the underlying step edges is several orders of magnitude larger than all of the other length scales in the problem, like wavelength, amplitude, and sheet length, it only adds negligibly small higher-order corrections to the classical scaling law.

We next turn to addressing some potential issues that can arise when imaging 2D materials on a tilted surface using STM. Tip artifacts are common when imaging 2D materials with STM, particularly because they tend to stick to the tip. However, such effects are generally more pronounced for unstretched micron-sized suspended sheets. The graphene sheet in our study should be much less susceptible to such behavior as it is under tension and is suspended only over a

very small region (tens of nanometers). Topographs taken in forward and backward scans, as well as under order of magnitude ranges of tunneling current (~100 pA to 1 nA), are similar, implying that graphene is not sticking to the tip. The experimentally measured rippling angle and its triangular shape (Figure 3d) are also found consistent with atomistic simulations (presented later in Figure 4h), further supporting that tip artifacts are negligible in the experimental data. Imaging a tilted region, like the draped region, can also create artifacts as the standard technique of plane subtraction can lead to artificial compression. Instead, we rotate the coordinate system to extract accurate lengths on draped graphene (Supporting Information, Section 7).

To understand the origin of these nonclassical mechanical properties, we performed atomistic scale calculations of a graphene sheet draped over a curved Cu step edge (Figure 4). While density functional theory (DFT) calculations are widely used to model graphene structures,^{34–38} such simulations are computationally expensive and not feasible for modeling a graphene sheet suspended over a Cu step edge, which requires consideration of at least a few thousand atoms. On the other hand, none of the widely used classical force fields—which are generally suitable for simulating large systems—such as AMBER, 39 CHARMM, 40 GROMOS, 41 or OPLS, 42 can be used to correctly reproduce the mechanical properties of graphene while simultaneously satisfying chemically justified carbon-copper interactions. Fortunately, a recently developed Cu-C ReaxFF parameter set⁴³ can be used to model a graphene sheet at a copper step edge, as it not only includes the parameters for interactions between carbon atoms that correctly describe the mechanical properties of graphene but has also been shown to accurately model experimentally observed draping of a suspended graphene ribbon at a copper step.44 Thus, we used the ReaxFF method with a recently updated version of this parameter set to further stabilize the carbon-copper interactions to perform atomistic simulations and understand the mechanical properties of our system. See the Supporting Information, Section 3 for more information on the ReaxFF simulations performed. All presented simulation snapshots were visualized using visual molecular dynamics (VMD)⁴⁵ or the Schrodinger package, 46 while all atomistic simulations were performed with the use of the ADF software.4

As the ripples are observed to form preferentially on curved step edges (Figure 2c,d), we model them by generating a series of Cu steps of varying height h and curvature (Figure 4a) and placing 8 nm square graphene sheets near them (Figure 4b). All considered structures were first energy-minimized, proceeded by a series of NPT (i.e., keeping the number of particles, the pressure, and temperatures constant) simulations. The sheet temperature was initially set to 5 K to allow the graphene to slowly connect with the Cu substrate. Then, to facilitate deformations of the graphene sheet including additional attachment to the substrate, the sheet temperature was raised to 175 K. After 15 ps, the graphene formed visible ripples for all considered systems. In Figure 4c, the final structure for one such model (described as model A in the Supporting Information, Section 3) with a step height of 1.6 nm is presented. Unlike the STM data, where it is not possible to see underneath the graphene sheet, for the simulated system, we can create a cut-away view (Figure 4d), highlighting the suspension of the graphene in the draped region. Thus, the simulation implies that ripples similar to those experimentally

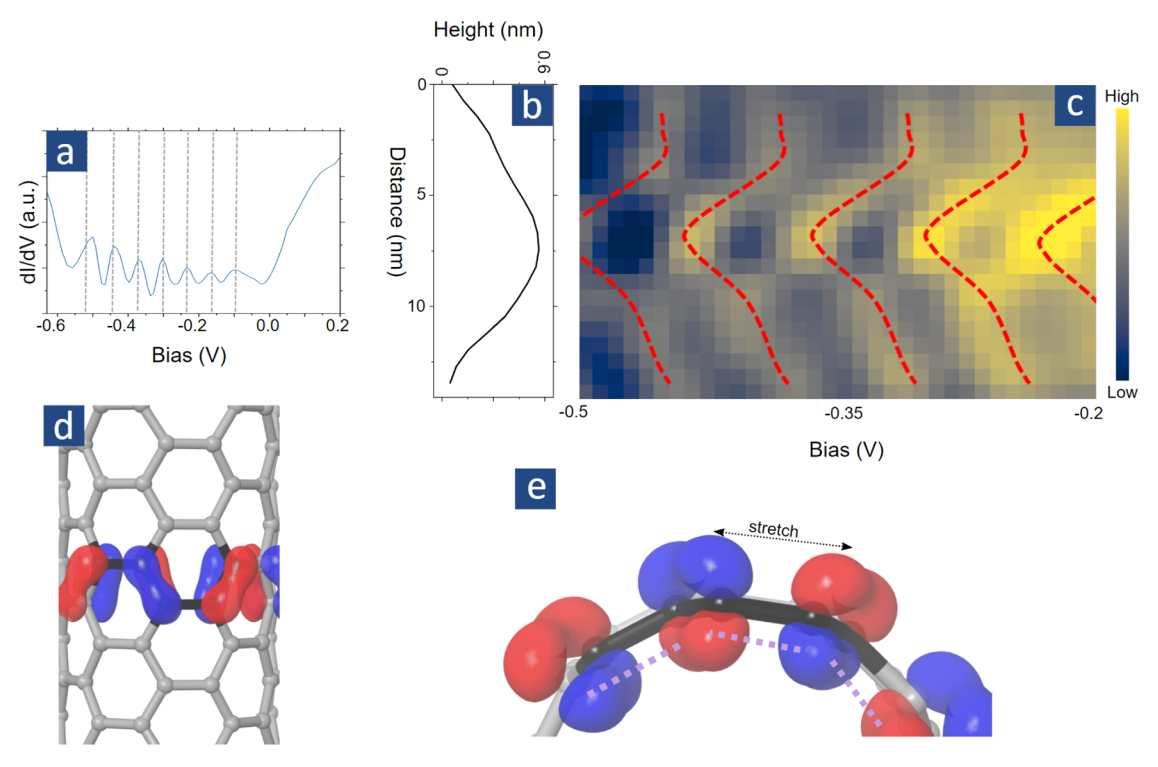


Figure 5. Origin of nonclassical ripples: (a) measuring the LDOS by scanning tunneling spectra taken on rippled graphene shows a series of equidistant peaks marked by gray dashed lines due to the formation of strain-modulated superlattices. ⁴⁹ Near ripple extrema with height profile shown in (b), the equidistant LDOS peaks shift toward negative bias as marked by red dashed lines in (c). Such a simultaneous shift of all of the peaks is the result of shifting of the Dirac point, corroborating that graphene is indeed stretched at the ripple crest. For plot in (c), 100 individual spectra were taken at each spatial point and averaged. When the graphene lattice is bent under curvature (d) top and (e) side views, the p_z orbitals (shown by red and blue lobes with the colors corresponding to electronic spin) get closer than what they were in a flat graphene sheet, forcing them to interact (purple dashed lines). Then, the optimal configuration of graphene is where the local bond lengths are stretched to reduce p_z-p_z orbital interaction. This local stretching of the bonds at ripple crests makes it behave unlike a thin classical fabric. These out-of-plane and in-plane modes of deformation occur simultaneously to create a strain-locked optimal buckling configuration in draped graphene sheets.

observed can be induced in graphene just by draping it on a curved Cu step edge (analogous to a draped tablecloth) and does not require the formation of any vicinal surface reconstructions in the substrate, which might occur at high growth temperatures.³² We note that even if the flat terraces are not perfectly uniform, the simulation implies that these small substrate imperfections are not required in forming ripples or determining the ultimate shape of rippled graphene.

Next, we compare the shape of the ripples obtained from these simulations and find them to be consistent with experimental observations. To better visualize the shape of the rippled graphene sheet, in Figure 4e, we make all carbon atoms translucent except for a line of atoms across the ripple highlighted in cyan. In the extracted profile of these highlighted atoms (Figure 4f), we see that these simulated ripples are also triangular (as highlighted by black dashed linear guides to the eye) rather than sinusoidal, with an apex angle of 170° ($\pm 2^{\circ}$) across all considered systems (Table T2 in the Supporting Information, Section 3), consistent with the experimentally measured value of 168° (±3°). Furthermore, profiles extracted from two different simulated systems show that it is possible to have ripples with similar sheet lengths (Figure 4g) but very different ripple wavelengths (Figure 4h here $\lambda_A \approx 1.5 \lambda_B$). We also tested the system with a rotated graphene sheet to confirm that chirality does not play a significant role in determining the ripple shapes (Figure S2 in the Supporting Information, Section 3). Thus, our simulations

accurately describe the observed mechanical properties of these nanometer wavelength ripples in draped graphene.

With simulations capturing the essential physics of the system, we next try to understand these remarkable observations. In particular, we try to understand exactly which parts of classical rippling theory fail when applied to a graphene sheet and why. One of the advantages of our simulation approach is the possibility of selectively switching off particular interactions to assess how important they are for a given phenomenon to occur. As elaborated further in the Supporting Information Section 4, we find that switching off dihedral interactions immediately leads to the disappearance of these ripples (Figure S3). The dihedral interaction, which is necessary to correctly describe the presence of conjugated π bonds, captures the effect of bending a discrete lattice and hence it is only natural that it plays a crucial role in determining the shape of the ripples. Lu et al. 48 found that the dihedral interaction is important in determining the bending modulus of monolayer graphene. In particular, they hypothesized using theoretical calculations that carbon nanotubes must stretch in the tangential direction when they are rolled from a graphene sheet, increasing their radius.

These two observations that ripples are eliminated when dihedral interactions are turned off and that dihedral interactions can result in transverse stretching of the bonds suggest that this transverse in-plane stretching is likely a crucial component missing from the classical theory of rippling. The classical theory only considers out-of-plane bending, and that

may lead to incorrect predictions when applied to ripple structures in graphene (and likely other 2D materials). Moreover, such in-plane stretching, should it exist, would likely occur only where graphene is bent, that is, as the ripples are triangular, in a very narrow region at the crest of each ripple. Such a strain variation over a very narrow region is challenging to resolve using direct atomic imaging techniques. For example, though such an in-plane mode of deformation was also proposed by Tapaszto et. al. 13 to account for the breakdown of the classical rippling theory, direct experimental evidence of the same and measurement of this in-plane strain and its spatial variation has not been achieved. For that, we turn to measuring electronic properties, which should be affected by this local stretching to provide indirect evidence of in-plane stretching of bonds at ripple extrema. Electronic properties are dependent on the overlap of electronic wavefunctions of nearest neighbor atoms and are hence exponentially more sensitive than STM topography to bond length distortions.

In Figure 5a, we show the local density of states (LDOS) measured on rippled graphene, where, in addition to the Vshape of the Dirac cone, we see a series of equidistant peaks. Details of the equal energy-spaced peak structure, resulting from modulated pseudomagnetic fields, are discussed in ref 49. Briefly, we found that the familiar $E_n \propto \sqrt{n}$ Landau quantization only holds when the pseudomagnetic field profile is uniform. In the present case, the ripples periodically modulate the pseudomagnetic field, changing it over a length scale that is comparable to the magnetic length. This periodically varying pseudomagnetic field results in a novel quantization with equidistant LDOS peaks. In addition to the spatially periodic pseudomagnetic fields, local stretching of the bonds at ripple extrema should also result in a pseudo-electric field there. 50 This pseudo-electric field should shift the entire tunneling spectrum, and its effect can be visualized by tracking the shift of the LDOS peaks near ripple extrema. The LDOS peaks are most prominent for negative biases, with the asymmetry arising likely due to the next nearest neighbor hopping in a strained lattice.⁵¹ We focus only on those bias values for our next analysis. Plotting the LDOS at each point of a linecut profile near a ripple crest (Figure 5b,c), we see that the equidistant peaks (marked by red dashed lines) shift in unison toward negative bias, implying a shift of the Dirac point (DP). Such a DP shift is known to occur due to changing the local scalar potential and reduced Fermi velocity when graphene is stretched. 50,52-54 Following Guinea et al.,55 we use this DP shift to estimate strain at the ripple crest. A onedimensional stretching of the lattice u_{xx} creates a scalar potential $V = V_0 u_{xx}$ where $V_0 \approx 3$ eV. A DP shift of roughly 100 meV over 3 nm implies a pseudo-electric field of strength $|E| = \frac{100 \text{ meV}}{3 \text{ nm}} = 3 \times 10^7 \frac{\text{V}}{\text{m}}$, suggesting a transverse stretching of about $u_{xx} = \frac{|E| x}{V_0} = 3\%$. Notably, this pseudo-electric field magnitude is comparable to E-fields in the smallest operational p-n junctions. 56,57 We also note that a change in the surface area resulting from in-plane deformations in rippled graphene like the one observed here was also predicted in calculations by Qin et al.58

Qin et al.⁵⁸
A possible origin for this transverse in-plane stretching is explained in Figure 5d,e. Graphene consists of sp²-bonded carbon atoms with the p_z orbitals sticking out of plane. For a flat graphene sheet, these p_z orbitals have minimal overlap.

However, a bent graphene sheet can force these p, orbitals to interact. By local in-plane stretching of the bonds, the distance between the p_z orbitals can be increased, and hence graphene, unlike a thin classical fabric, suffers in-plane stretching when it is subjected to out-of-plane buckling. The local charge inhomogeneity resulting from such bending and the subsequent rehybridization of electronic orbitals should also help in stabilizing the ripples.⁵⁹ Numerous theoretical studies have treated in-plane and out-of-plane deformations of graphene to be independent, analogous to classical fabrics. Our results suggest that such an approach might be questionable at the nanometer length scale as these two modes of deformation are inherently tied together even for small out-of-plane deviations $(\sim 10^{\circ})$. In addition to the above analysis, based on rigorous atomistic calculations, in the Supporting Information, Section 5, we also present a simple phenomenological model to capture the mechanics of graphene bending. There, we show that the in-plane and out-of-plane modes of deformations compete with each other resulting in a strain-locked optimal buckling configuration.

We note that the ReaxFF calculations were performed for much smaller model systems than those observed experimentally. The largest simulated system had ~50 000 atoms with a Cu step edge height of only 1.6 nm, resulting in fewer and smaller ripples than those observed experimentally. Nevertheless, the fact that similar observations were made as in the experiments suggests that the essential physics of the system is adequately described even by such small systems. Furthermore, in the simulations, the graphene was placed near the curved Cu step edge, meaning that the dynamics of the growth process was neglected, which might also affect the final draping configuration. Large-scale ReaxFF simulations, using force-biased Monte Carlo, as previously employed for carbonnanotube growth in Ni-clusters, 63 may be able to capture these growth dynamics. Our observations also suggest that electronic interactions can affect the mechanical properties, forcing graphene to stretch at the ripple extrema (Figure 5). Electronic interactions, like electron transfer between Cu and graphene, are not explicitly accounted for in the ReaxFF method, but recent reports indicate⁶⁴ that perhaps e-ReaxFF might be able to include such effects. Finally, since our samples were grown at a relatively high temperature of 1020 °C on Cu foils, we most likely have a polycrystalline substrate and we believe that our observations reflect the inherent mechanical properties of graphene. However, we note that further measurements for the samples with the controlled crystal structure would be interesting.

CONCLUSIONS

We studied graphene sheets as they drape over Cu step edges and explained the formation of ripples that violate classical scaling laws. Unlike a thin classical sheet, we found that graphene undergoes stretching over a few bond lengths at ripple crests and troughs to reduce interactions between nearby \mathbf{p}_z orbitals. Interestingly, the effect of this stretching over a very narrow region is significant enough that even ripples much larger than unit cell dimensions (up to tens of nanometers, where one might be tempted to use a continuum approximation) differ fundamentally from classical fabrics. This observation should be considered carefully while developing strain-enabled and flexible electronics. Furthermore, the general nature of our arguments implies that other 2D materials should also form nonclassical ripples when forced

to buckle at the nanoscale. Suggestively, we note that triangular ripples have already been observed in WSe2 as well.65 The validity of the continuum elasticity theory will always be questionable when it is applied to a discrete lattice. Thus, based on our results, we expect other 2D materials with out-ofplane electronic distributions to also stretch like graphene when they bend resulting in nonclassical ripples. In contrast to our study of ripples with wavelengths measuring tens of nanometers, larger ripples, with wavelengths approaching the micron scale, have been shown to conform to the classical theory, 16 implying the existence of a crossover region where the bending mechanics of graphene should vary significantly. Such a variation, where the graphene sheet bends differently depending on the size of deformations, may help address the long-standing debate about the bending modulus of monolayer graphene. 3,66-68 Also interesting would be the exploration of how the hybridized p_z orbitals at the ripple crests can affect the local interlayer slipping and ultimately bending in multilayer graphene sheets. 69 The techniques developed in this paper to exert strain at the nanoscale and accurately modeling the effects of such should present a strong foundation for future work in understanding the mechanical properties of 2D materials and realizing the promise of straintronics.

ASSOCIATED CONTENT

Supporting Information

The Supporting Information is available free of charge at https://pubs.acs.org/doi/10.1021/acsanm.2c02137.

Methods, details of the sample growth; ReaxFF method; role of dihedral interactions; phenomenological model of graphene bending; measuring the radius of curvature at ripple crests; possible artifacts in imaging a tilted surface; transverse stretching at ripple, extrema from simulations; scaling laws for draped fabrics and more STM images of draped graphene (PDF)

AUTHOR INFORMATION

Corresponding Authors

Riju Banerjee — Department of Physics, The Pennsylvania State University, University Park, Pennsylvania 16802, United States; Present Address: James Franck Institute, University of Chicago, Chicago, Illinois 60637, United States; orcid.org/0000-0003-3454-6960; Email: rijubanerjee@uchicago.edu

E. W. Hudson – Department of Physics, The Pennsylvania State University, University Park, Pennsylvania 16802, United States; Email: ehudson@psu.edu

Authors

Tomotaroh Granzier-Nakajima – Department of Physics, The Pennsylvania State University, University Park, Pennsylvania 16802, United States

Aditya Lele – Department of Mechanical Engineering, The Pennsylvania State University, University Park, Pennsylvania 16802, United States

Jessica A. Schulze – Department of Chemistry, The Pennsylvania State University, University Park, Pennsylvania 16802, United States

Md Jamil Hossain — Department of Mechanical Engineering, The Pennsylvania State University, University Park, Pennsylvania 16802, United States; orcid.org/0000-0002-8737-2821 Wenbo Zhu — Department of Mechanical Engineering, The Pennsylvania State University, University Park, Pennsylvania 16802, United States

Lavish Pabbi — Department of Physics, The Pennsylvania State University, University Park, Pennsylvania 16802, United States

Malgorzata Kowalik – Department of Mechanical Engineering, The Pennsylvania State University, University Park, Pennsylvania 16802, United States

Adri C. T. van Duin – Department of Mechanical Engineering, The Pennsylvania State University, University Park, Pennsylvania 16802, United States; Department of Chemistry, The Pennsylvania State University, University Park, Pennsylvania 16802, United States; orcid.org/0000-0002-3478-4945

Mauricio Terrones — Department of Physics, The Pennsylvania State University, University Park, Pennsylvania 16802, United States: orcid.org/0000-0003-0010-2851

Complete contact information is available at: https://pubs.acs.org/10.1021/acsanm.2c02137

Author Contributions

R.B. conceived the project; T.G.N. prepared the samples; R.B., L.P. built the custom instrument; R.B., L.P. collected the data; R.B., E.W.H. analyzed the data; M.K., A.L., J.A.S., J.H., and W.Z. performed the atomistic simulations; R.B., T.G.N. did the phenomenological modeling; all authors took part in interpreting the results and writing the paper; and A.C.T.vD, M.T., and E.W.H. advised.

Funding

This material is based upon work supported by the National Science Foundation under Grant No. 1229138. T.G.N. and M.T. acknowledge The Air Force Office of Scientific Research (AFOSR) grant 17RT0244. A.L., J.A.S., J.M.H., W.Z., M.K., and A.C.T.v.D. acknowledge the financial support by the National Science Foundation (NSF) through the Pennsylvania State University 2D Crystal Consortium Materials Innovation Platform (2DCC-MIP) under the NSF cooperative agreements DMR-1808900, DMR-1539916, and DMR-2039351. Computations for this research were performed on the Pennsylvania State University's Institute for Computational and Data Sciences' Roar supercomputer. This content is solely the responsibility of the authors and does not necessarily represent the views of the Institute for Computational and Data Sciences.

Notes

The authors declare no competing financial interest.

REFERENCES

(1) Strutt, J. The Theory of Sound; Cambridge University Press, 2011.

(2) Zang, J.; Ryu, S.; Pugno, N.; Wang, Q.; Tu, Q.; Buehler, M. J.; Zhao, X. Multifunctionality and Control of the Crumpling and Unfolding of Large-Area Graphene. *Nat. Mater.* 2013, 12, 321–325.

(3) Blees, M. K.; Barnard, A. W.; Rose, P. A.; Roberts, S. P.; McGill, K. L.; Huang, P. Y.; Ruyack, A. R.; Kevek, J. W.; Kobrin, B.; Muller, D. A.; McEuen, P. L. Graphene Kirigami. *Nature* **2015**, *524*, 204–207.

(4) Miskin, M. Z.; Dorsey, K. J.; Bircan, B.; Han, Y.; Muller, D. A.; McEuen, P. L.; Cohen, I. Graphene-Based Bimorphs for Micron-Sized, Autonomous Origami Machines. *Proc. Natl. Acad. Sci. U.S.A.* **2018**, *115*, 466–470.

(5) Lee, W.; Liu, Y.; Lee, Y.; Sharma, B. K.; Shinde, S. M.; Kim, S. D.; Nan, K.; Yan, Z.; Han, M.; Huang, Y.; Zhang, Y.; Ahn, J.-H.; Rogers, J. A. Two-Dimensional Materials in Functional Three-

- Dimensional Architectures with Applications in Photodetection and Imaging. *Nat. Commun.* **2018**, *9*, No. 1417.
- (6) Xu, W.; Qin, Z.; Chen, C.-T.; Kwag, H. R.; Ma, Q.; Sarkar, A.; Buehler, M. J.; Gracias, D. H. Ultrathin Thermoresponsive Self-Folding 3D Graphene. *Sci. Adv.* **2017**, *3*, No. e1701084.
- (7) Lee, C.; Wei, X.; Kysar, J. W.; Hone, J. Measurement of the Elastic Properties and Intrinsic Strength of Monolayer Graphene. *Science* **2008**, *321*, 385–388.
- (8) Scarpa, F.; Adhikari, S.; Phani, A. S. Effective Elastic Mechanical Properties of Single Layer Graphene Sheets. *Nanotechnology* **2009**, *20*, No. 065709.
- (9) Scarpa, F.; Adhikari, S.; Gil, A. J.; Remillat, C. The Bending of Single Layer Graphene Sheets: The Lattice versus Continuum Approach. *Nanotechnology* **2010**, *21*, No. 125702.
- (10) Zhang, D.-B.; Akatyeva, E.; Dumitrică, T. Bending Ultrathin Graphene at the Margins of Continuum Mechanics. *Phys. Rev. Lett.* **2011**, *106*, No. 255503.
- (11) Shenderova, O. A.; Zhirnov, V. V.; Brenner, D. W. Carbon Nanostructures. Crit. Rev. Solid State Mater. Sci. 2002, 27, 227–356.
- (12) Huang, Y.; Wu, J.; Hwang, K. C. Thickness of Graphene and Single-Wall Carbon Nanotubes. *Phys. Rev. B* **2006**, *74*, No. 245413.
- (13) Tapasztó, L.; Dumitrică, T.; Kim, S. J.; Nemes-Incze, P.; Hwang, C.; Biró, L. P. Breakdown of Continuum Mechanics for Nanometre-Wavelength Rippling of Graphene. *Nat. Phys.* **2012**, *8*, 739–742.
- (14) Cerda, E.; Mahadevan, L. Geometry and Physics of Wrinkling. *Phys. Rev. Lett.* **2003**, *90*, No. 074302.
- (15) Bai, K.-K.; Zhou, Y.; Zheng, H.; Meng, L.; Peng, H.; Liu, Z.; Nie, J.-C.; He, L. Creating One-Dimensional Nanoscale Periodic Ripples in a Continuous Mosaic Graphene Monolayer. *Phys. Rev. Lett.* **2014**, *113*, No. 086102.
- (16) Bao, W.; Miao, F.; Chen, Z.; Zhang, H.; Jang, W.; Dames, C.; Lau, C. N. Controlled Ripple Texturing of Suspended Graphene and Ultrathin Graphite Membranes. *Nat. Nanotechnol.* **2009**, *4*, 562–566.
- (17) Fasolino, A.; Los, J. H.; Katsnelson, M. I. Intrinsic Ripples in Graphene. *Nat. Mater.* **2007**, *6*, 858–861.
- (18) Meyer, J. C.; Geim, A. K.; Katsnelson, M. I.; Novoselov, K. S.; Booth, T. J.; Roth, S. The Structure of Suspended Graphene Sheets. *Nature* **2007**, *446*, 60–63.
- (19) Mermin, N. D. Crystalline Order in Two Dimensions. *Phys. Rev.* **1968**, *176*, 250–254.
- (20) Kang, J. H.; Moon, J.; Kim, D. J.; Kim, Y.; Jo, I.; Jeon, C.; Lee, J.; Hong, B. H. Strain Relaxation of Graphene Layers by Cu Surface Roughening. *Nano Lett.* **2016**, *16*, 5993–5998.
- (21) Xu, K.; Cao, P. G.; Heath, J. R. Scanning Tunneling Microscopy Characterization of the Electrical Properties of Wrinkles in Exfoliated Graphene Monolayers. *Nano Lett.* **2009**, *9*, 4446–4451.
- (22) Teague, M. L.; Lai, A. P.; Velasco, J.; Hughes, C. R.; Beyer, A. D.; Bockrath, M. W.; Lau, C. N.; Yeh, N.-C. Evidence for Strain-Induced Local Conductance Modulations in Single-Layer Graphene on SiO 2. *Nano Lett.* **2009**, *9*, 2542–2546.
- (23) Li, S.-Y.; Zhou, M.; Qiao, J.-B.; Duan, W.; He, L. Wide-Band-Gap Wrinkled Nanoribbon-like Structures in a Continuous Metallic Graphene Sheet. *Phys. Rev. B* **2016**, *94*, No. 085419.
- (24) Yan, H.; Chu, Z.-D.; Yan, W.; Liu, M.; Meng, L.; Yang, M.; Fan, Y.; Wang, J.; Dou, R.-F.; Zhang, Y.; Liu, Z.; Nie, J.-C.; He, L. Superlattice Dirac Points and Space-Dependent Fermi Velocity in a Corrugated Graphene Monolayer. *Phys. Rev. B* **2013**, *87*, No. 075405.
- (25) Meng, L.; He, W.-Y.; Zheng, H.; Liu, M.; Yan, H.; Yan, W.; Chu, Z.-D.; Bai, K.; Dou, R.-F.; Zhang, Y.; Liu, Z.; Nie, J.-C.; He, L. Strain-Induced One-Dimensional Landau Level Quantization in Corrugated Graphene. *Phys. Rev. B* **2013**, *87*, No. 205405.
- (26) Klimov, N. N.; Jung, S.; Zhu, S.; Li, T.; Wright, C. A.; Solares, S. D.; Newell, D. B.; Zhitenev, N. B.; Stroscio, J. A. Electromechanical Properties of Graphene Drumheads. *Science* **2012**, *336*, 1557–1561.
- (27) Gill, S. T.; Hinnefeld, J. H.; Zhu, S.; Swanson, W. J.; Li, T.; Mason, N. Mechanical Control of Graphene on Engineered Pyramidal Strain Arrays. *ACS Nano* **2015**, *9*, 5799–5806.

- (28) de Parga, A. L. V.; Calleja, F.; Borca, B.; Passeggi, M. C. G.; Hinarejos, J. J.; Guinea, F.; Miranda, R. Periodically Rippled Graphene: Growth and Spatially Resolved Electronic Structure. *Phys. Rev. Lett.* **2008**, *100*, No. 056807.
- (29) Cerda, E.; Mahadevan, L.; Pasini, J. M. The Elements of Draping. *Proc. Natl. Acad. Sci. U.S.A.* **2004**, *101*, 1806–1810.
- (30) Hayashi, K.; Sato, S.; Yokoyama, N. Anisotropic Graphene Growth Accompanied by Step Bunching on a Dynamic Copper Surface. *Nanotechnology* **2013**, 24, No. 025603.
- (31) Yi, D.; Luo, D.; Wang, Z.-J.; Dong, J.; Zhang, X.; Willinger, M.-G.; Ruoff, R. S.; Ding, F. What Drives Metal-Surface Step Bunching in Graphene Chemical Vapor Deposition. *Phys. Rev. Lett.* **2018**, *120*, No. 246101.
- (32) Tian, J.; Cao, H.; Wu, W.; Yu, Q.; Guisinger, N. P.; Chen, Y. P. Graphene Induced Surface Reconstruction of Cu. *Nano Lett.* **2012**, 12, 3893–3899.
- (33) Zhang, C.; Lu, C.; Pei, L.; Li, J.; Wang, R. The Wrinkling and Buckling of Graphene Induced by Nanotwinned Copper Matrix: A Molecular Dynamics Study. *Nano Mater. Sci.* **2021**, *3*, 95–103.
- (34) Banerjee, S.; Bhattacharyya, D. Electronic Properties of Nano-Graphene Sheets Calculated Using Quantum Chemical DFT. *Comput. Mater. Sci.* **2008**, *44*, 41–45.
- (35) Cicero, G.; Grossman, J. C.; Schwegler, E.; Gygi, F.; Galli, G. Water Confined in Nanotubes and between Graphene Sheets: A First Principle Study. *J. Am. Chem. Soc.* **2008**, *130*, 1871–1878.
- (36) Lusk, M. T.; Carr, L. D. Nanoengineering Defect Structures on Graphene. *Phys. Rev. Lett.* **2008**, *100*, No. 175503.
- (37) Nakada, K.; Ishii, A. Migration of Adatom Adsorption on Graphene Using DFT Calculation. *Solid State Commun.* **2011**, *151*, 13–16
- (38) Rani, P.; Dubey, G. S.; Jindal, V. K. DFT Study of Optical Properties of Pure and Doped Graphene. *Phys. E* **2014**, *62*, 28–35.
- (39) Case, D. A.; Belfon, K.; Ben-Shalom, I. Y.; Brozell, S. R.; Cerutti, D. S.; Cheatham, T. E., III; Cruzeiro, V.W.D.; Darden, T. A.; Duke, R. E.; Giambasu, G.; Gilson, M. K.; Gohlke, H.; Goetz, A. W.; Harris, R.; Izadi, S.; Izmailov, S. A.; Kasavajhala, K.; Kovalenko, A.; Krasny, R.; Kurtzman, T.; Lee, T. S.; LeGrand, S.; Li, P.; Lin, C.; Liu, J.; Luchko, T.; Luo, R.; Man, V.; Merz, K. M.; Miao, Y.; Mikhailovskii, O.; Monard, G.; Nguyen, H.; Onufriev, A.; Pan, F.; Pantano, S.; Qi, R.; Roe, D. R.; Roitberg, A.; Sagui, C.; Schott-Verdugo, S.; Shen, J.; Simmerling, C. L.; Skrynnikov, N. R.; Smith, J.; Swails, J.; Walker, R. C.; Wang, J.; Wilson, L.; Wolf, R. M.; Wu, X.; Xiong, Y.; Xue, Y.; York, D. M.; Kollman, P. A. AMBER 2020; University of California: San Francisco, 2020.
- (40) Jo, S.; Kim, T.; Iyer, V. G.; Im, W. CHARMM-GUI: A Web-Based Graphical User Interface for CHARMM. J. Comput. Chem. **2008**, 29, 1859–1865.
- (41) Scott, W. R. P.; Hünenberger, P. H.; Tironi, I. G.; Mark, A. E.; Billeter, S. R.; Fennen, J.; Torda, A. E.; Huber, T.; Krüger, P.; van Gunsteren, W. F. The GROMOS Biomolecular Simulation Program Package. *J. Phys. Chem. A* **1999**, *103*, 3596–3607.
- (42) Robertson, M. J.; Tirado-Rives, J.; Jorgensen, W. L. Improved Peptide and Protein Torsional Energetics with the OPLS-AA Force Field. J. Chem. Theory Comput. 2015, 11, 3499–3509.
- (43) Zhu, W.; Gong, H.; Han, Y.; Zhang, M.; van Duin, A. C. T. Development of a Reactive Force Field for Simulations on the Catalytic Conversion of C/H/O Molecules on Cu-Metal and Cu-Oxide Surfaces and Application to Cu/CuO-Based Chemical Looping. *J. Phys. Chem. C* **2020**, *124*, 12512–12520.
- (44) Kowalik, M.; Hossain, M. J.; Lele, A.; Zhu, W.; Banerjee, R.; Granzier-Nakajima, T.; Terrones, M.; Hudson, E. W.; van Duin, A. C. T. Atomistic-Scale Simulations on Graphene Bending Near a Copper Surface. *Catalysts* **2021**, *11*, No. 208.
- (45) Humphrey, W.; Dalke, A.; Schulten, K. VMD: Visual Molecular Dynamics. *J. Mol. Graphics* **1996**, *14*, 33–38.
- (46) Schrödinger Release 2019-4 Jaguar; Schrödinger, LLC: New York, NY, 2021.
- (47) Chemistry, S.T.ADF Modeling Suite; Vrije Universiteit: Amsterdam, The Netherlands, 2017.

- (48) Lu, Q.; Arroyo, M.; Huang, R. Elastic Bending Modulus of Monolayer Graphene. J. Phys. D: Appl. Phys. 2009, 42, No. 102002.
- (49) Banerjee, R.; Nguyen, V.-H.; Granzier-Nakajima, T.; Pabbi, L.; Lherbier, A.; Binion, A. R.; Charlier, J.-C.; Terrones, M.; Hudson, E. W. Strain Modulated Superlattices in Graphene. Nano Lett. 2020, 20, 3113-3121.
- (50) Suzuura, H.; Ando, T. Phonons and Electron-Phonon Scattering in Carbon Nanotubes. Phys. Rev. B 2002, 65, No. 235412.
- (51) Bai, K.-K.; Wei, Y.-C.; Qiao, J.-B.; Li, S.-Y.; Yin, L.-J.; Yan, W.; Nie, J.-C.; He, L. Detecting Giant Electron-Hole Asymmetry in a Graphene Monolayer Generated by Strain and Charged-Defect Scattering via Landau Level Spectroscopy. Phys. Rev. B 2015, 92, No. 121405.
- (52) Huang, M.; Yan, H.; Heinz, T. F.; Hone, J. Probing Strain-Induced Electronic Structure Change in Graphene by Raman Spectroscopy. Nano Lett. 2010, 10, 4074-4079.
- (53) Choi, S.-M.; Jhi, S.-H.; Son, Y.-W. Effects of Strain on Electronic Properties of Graphene. Phys. Rev. B 2010, 81, No. 081407. (54) Oliva-Leyva, M.; Naumis, G. G. Generalizing the Fermi Velocity of Strained Graphene from Uniform to Nonuniform Strain. Phys. Lett. A 2015, 379, 2645-2651.
- (55) Guinea, F.; Geim, A. K.; Katsnelson, M. I.; Novoselov, K. S. Generating Quantizing Pseudomagnetic Fields by Bending Graphene Ribbons. Phys. Rev. B 2010, 81, No. 035408.
- (56) Lu, W.; Lee, Y.; Murdzek, J.; Gertsch, J.; Vardi, A.; Kong, L.; George, S. M.; del Alamo, J. A. In First Transistor Demonstration of Thermal Atomic Layer Etching: InGaAs FinFETs with Sub-5 nm Fin-Width Featuring in situ ALE-ALD, IEEE International Electron Devices Meeting (IEDM); IEEE, 2018.
- (57) Neaman, D. Semiconductor Physics And Devices; McGraw-Hill, 2012.
- (58) Qin, Z.; Taylor, M.; Hwang, M.; Bertoldi, K.; Buehler, M. J. Effect of Wrinkles on the Surface Area of Graphene: Toward the Design of Nanoelectronics. Nano Lett. 2014, 14, 6520-6525.
- (59) Kim, E.-A.; Neto, A. H. C. Graphene as an Electronic Membrane. EPL (Europhys. Lett.) 2008, 84, No. 57007.
- (60) Wei, Y.; Wang, B.; Wu, J.; Yang, R.; Dunn, M. L. Bending Rigidity and Gaussian Bending Stiffness of Single-Layered Graphene. Nano Lett. 2013, 13, 26-30.
- (61) Wu, Y.; Zhai, D.; Pan, C.; Cheng, B.; Taniguchi, T.; Watanabe, K.; Sandler, N.; Bockrath, M. Quantum Wires and Waveguides Formed in Graphene by Strain. Nano Lett. 2018, 18, 64-69.
- (62) Castle, T.; Cho, Y.; Gong, X.; Jung, E.; Sussman, D. M.; Yang, S.; Kamien, R. D. Making the Cut: Lattice Kirigami Rules. Phys. Rev. Lett. 2014, 113, No. 245502.
- (63) Neyts, E. C.; Shibuta, Y.; van Duin, A. C. T.; Bogaerts, A. Catalyzed Growth of Carbon Nanotube with Definable Chirality by Hybrid Molecular Dynamics-Force Biased Monte Carlo Simulations. ACS Nano 2010, 4, 6665-6672.
- (64) Leven, I.; Hao, H.; Tan, S.; Guan, X.; Penrod, K. A.; Akbarian, D.; Evangelisti, B.; Hossain, M. J.; Islam, M. M.; Koski, J. P.; Moore, S.; Aktulga, H. M.; van Duin, A. C. T.; Head-Gordon, T. Recent Advances for Improving the Accuracy, Transferability, and Efficiency of Reactive Force Fields. J. Chem. Theory Comput. 2021, 17, 3237-
- (65) Xie, S.; Tu, L.; Han, Y.; Huang, L.; Kang, K.; Lao, K. U.; Poddar, P.; Park, C.; Muller, D. A.; DiStasio, R. A.; Park, J. Coherent, Atomically Thin Transition-Metal Dichalcogenide Superlattices with Engineered Strain. Science 2018, 359, 1131-1136.
- (66) Akinwande, D.; Brennan, C. J.; Bunch, J. S.; Egberts, P.; Felts, J. R.; Gao, H.; Huang, R.; Kim, J.-S.; Li, T.; Li, Y.; Liechti, K. M.; Lu, N.; Park, H. S.; Reed, E. J.; Wang, P.; Yakobson, B. I.; Zhang, T.; Zhang, Y.-W.; Zhou, Y.; Zhu, Y. A Review on Mechanics and Mechanical Properties of 2D Materials-Graphene and Beyond. Extreme Mech. Lett. 2017, 13, 42-77.
- (67) Lindahl, N.; Midtvedt, D.; Svensson, J.; Nerushev, O. A.; Lindvall, N.; Isacsson, A.; Campbell, E. E. B. Determination of the Bending Rigidity of Graphene via Electrostatic Actuation of Buckled Membranes. Nano Lett. 2012, 12, 3526-3531.

- (68) Košmrlj, A.; Nelson, D. R. Response of Thermalized Ribbons to Pulling and Bending. Phys. Rev. B 2016, 93, No. 125431.
- (69) Han, E.; Yu, J.; Annevelink, E.; Son, J.; Kang, D. A.; Watanabe, K.; Taniguchi, T.; Ertekin, E.; Huang, P. Y.; van der Zande, A. M. Ultrasoft Slip-Mediated Bending in Few-Layer Graphene. Nat. Mater. **2020**, 19, 305-309.

□ Recommended by ACS

One-Dimensional Strain Solitons Manipulated Superlubricity on Graphene Interface

Huizhong Bai, Fei Ma, et al.

AUGUST 01 2022

THE JOURNAL OF PHYSICAL CHEMISTRY LETTERS

READ 2

First-Principles Calculations on Janus MoSSe/Graphene van der Waals Heterostructures: Implications for Electronic **Devices**

Yuanfan Wang, Quan Xie, et al.

JUNE 07, 2022

ACS APPLIED NANO MATERIALS

READ **C**

Experimental Observation of ABCB Stacked Tetralayer Graphene

Konstantin G. Wirth, Thomas Taubner, et al.

OCTOBER 07, 2022

ACS NANO

RFAD 17

Topological Stone-Wales Defects Enhance Bonding and Electronic Coupling at the Graphene/Metal Interface

Benedikt P. Klein, J. Michael Gottfried, et al.

AUGUST 02, 2022

ACS NANO

READ **C**

Get More Suggestions >